NRC Research Press

ARTICLE

Air–water flow measurements in a flat slope pooled stepped waterway

S. Felder and H. Chanson

Abstract: Air–water flows on stepped spillways were investigated experimentally in the last decades with a focus on steep slope chutes equipped with flat horizontal steps. Detailed air–water flow properties were recorded herein with three stepped geometries down a slope of $\theta = 8.9°$ with: flat horizontal steps, pooled steps, and a combination of flat and pooled steps. The data included the distributions of basic air–water flow properties, as well as the energy dissipation and flow resistance data deduced from the air–water flow measurements. The results on the flat slope showed that the pooled stepped design enabled a greater rate of energy dissipation, but the pooled stepped geometries were affected by some flow instabilities and unsteady flow processes for a range of flow rates.

Key words: air–water flows, turbulence, stepped spillways, pooled steps, flow instabilities, physical modelling, turbulent energy dissipation.

Résumé : De nombreuses recherches ont été conduites pour étudier l'entrainement d'air sur des coursiers en marches d'escalier durant les dernières décennies. Ces travaux ont étudié principalement des géométries avec fortes pentes et des marches plates et horizontales. Ici, on présente de nouveaux travaux expérimentaux sur une faible pente ($\theta = 8{,}9°$) avec trois configurations : marches plates et horizontales, marches avec murets, et combinaison de marches plates et avec murets. Des mesures diphasiques détaillées ont été conduites. Les résultats indiquent que la dissipation d'énergie est maximum en présence de marches avec murets (en continue ou en alternance), mais ces géométries sont sujettes à des instabilités hydrodynamiques très importantes.

Mots-clés : entrainement d'air, turbulence, coursier en marches d'escalier, marches avec murets, instabilités hydrodynamiques, modélisation physique, dissipation d'énergie.

Introduction

Air–water flows on stepped spillways were investigated experimentally in the last two decades (e.g., Chanson 1993, 2001; Ruff and Frizell 1994; Chamani and Rajaratnam 1999; Carosi and Chanson 2008). Most research focused on the air–water flow properties down relatively steep slopes equipped with flat horizontal steps, and only a few studies investigated the air–water flows on pooled stepped spillways (Table 1). Kökpinar (2004) conducted some experiments on a stepped spillway with a slope of 30° with three different configurations: flat, pooled, and combination of flat and pooled steps. A similar study was conducted by André (2004) who investigated further pooled stepped spillway configurations with two channel slopes. A study of self-induced instabilities on pooled stepped spillways with slopes of $\theta = 8.9°$ and 14.6° was conducted by Thorwarth (2008). Thorwarth's work was motivated by some incident on the Sorpe Dam pooled stepped spillway, which was documented and illustrated by Chanson (2001) and Thorwarth (2008).

It is the purpose of this study to investigate thoroughly the air–water flow properties in a flat pooled stepped waterway. New measurements were conducted in a relatively large-size facility ($\theta = 8.9°$, $h = 0.05$ m, $L = 12$ m) with a double-tip phase-detection intrusive probe, where L is the length of the test section. Detailed air–water flow properties were recorded systematically for several flow rates with flat horizontal steps, pooled steps, and a combination of flat and pooled steps (Fig. 1). The results included the distributions of basic air–water flow properties, as well as the energy dissipation and flow resistance data. They showed that the pooled stepped design enabled a greater rate of energy dissipation for a flat slope ($\theta = 8.9°$ herein), but some flow instabilities may occur.

Experimental setup

New experiments were performed in a large size flat slope stepped spillway model at the Institute of Hydraulic Engineering and Water Resources Management (IWW) of RWTH Aachen University (Germany). The facility was 12 m long overall. The water entered the test section through an uncontrolled 0.50 m wide broad-crested weir followed by 21 identical steps made out of PVC with step width $W = 0.50$ m, step heights $h = 0.05$ m and step length $l = 0.319$ m; i.e., a channel slope $\theta = 8.9°$ (Figs. 1 and 2). The water discharge was measured using a sharp-crested weir at the downstream end of the flume. More details about the experimented facility were described by Felder et al. (2012) and Thorwarth (2008) who used the same facility.

Phase detection intrusive probe and signal processing

The air–water flow measurements were performed using a double-tip conductivity probe. The probe had an inner diameter Ø = 0.13 mm for both tips that were separated in the streamwise direction by $\Delta x = 5.1$ mm and in transverse direction by $\Delta z = 1$ mm. Such a probe was previously used by Thorwarth (2008) and Bung (2009). The translation of the phase-detection probe in the vertical direction was controlled by a trolley system equipped with an isel® control device.

All measurements were conducted at a sampling rate of 20 kHz per probe tip for 45 s. The air–water flow properties included the void fraction C (i.e., air concentration), the bubble count rate F defined as the number of bubbles/droplets detected by a leading

Received 21 October 2012. Accepted 19 March 2013.

S. Felder and H. Chanson. School of Civil Engineering, The University of Queensland, Brisbane QLD 4072, Australia.
Corresponding author: H. Chanson (e-mail: h.chanson@uq.edu.au).

Table 1. Experimental investigations of air–water flows on pooled stepped spillways.

Reference (1)	θ [°] (2)	Step geometry (3)	Flow conditions (4)	Instrumentation (5)	Comment (6)
Kökpinar (2004)	30	Flat steps: h = 6 cm, l = 10.4 cm Pooled steps: h = 6 cm, l = 10.4 cm, w = 3 cm, l_w = 2.6 cm Combination of flat/pooled steps: h = 6 cm, l = 10.4 cm, w = 3 cm, l_w = 2.6 cm	Q = 0.03–0.100 m^3/s, Re = 2.4×10^5–8.0×10^5	Double-tip fibre-optical probe (Ø = 0.08 mm)	W = 0.5 m, 64 steps
André (2004)	18.6	Flat steps: h = 6 cm, l = 17.8 cm Pooled steps: h = 6 cm, l = 17.8 cm, w = 3 cm, l_w = 2.6 cm Combination of flat/pooled steps: h = 6 cm, l = 17.8 cm, w = 3 cm, l_w = 2.6 cm	Q = 0.02–0.130 m^3/s, Re = 1.6×10^5–1.0×10^6	Double-tip fibre-optical probe (Ø = 0.08 mm)	W = 0.5 m, 42/64 steps
	30	Flat steps: h = 6 cm, l = 10.4 cm Pooled steps: h = 6 cm, l = 10.4 cm, w = 3 cm Combination of flat/pooled steps: h = 6 cm, l = 10.4 cm, w = 3 cm			
Thorwarth (2008)	8.9 14.6	Pooled steps: h = 5 cm, l = 31.9 cm, w = 0–5 cm Pooled steps: h = 5 cm, l = 19.2 cm, w = 0–5 cm, l_w = 1.5 cm	Q = 0.025–0.117 m^3/s, Re = 2.0×10^5–9.3×10^5	Double-tip conductivity probe (Ø = 0.13 mm)	W = 0.5 m, 22/26 steps
Present study	8.9	Flat steps: h = 5 cm, l = 31.9 cm	Q = 0.018–0.117 m^3/s, d_c/h = 1.0–3.55, Re = 1.4×10^5–9.3×10^5	Double-tip conductivity probe (Ø = 0.13 mm)	W = 0.5 m, 21 steps
		Pooled steps: h = w = 5 cm, l = 31.9 cm, l_w = 1.5 cm	Q = 0.027– 0.117 m^3/s, d_c/h = 1.35–3.55, Re = 2.2×10^5–9.3×10^5		
		Combination of flat/pooled steps: h = w = 5 cm, l = 31.9 cm, l_w = 1.5 cm	Q = 0.027–0.117 m^3/s, d_c/h = 1.35–3.55, Re = 2.2×10^5–9.3×10^5		

Note: θ, channel slope; d_c, critical flow depth; h, step height; l, step length; l_w, pool weir length; Q, water discharge; Re, Reynolds number defined in terms of the hydraulic diameter; w, pool weir height; W, channel width; ϕ, probe sensor size.

Fig. 1. Sketch of stepped spillway configurations (present study, $\theta = 8.9°$).

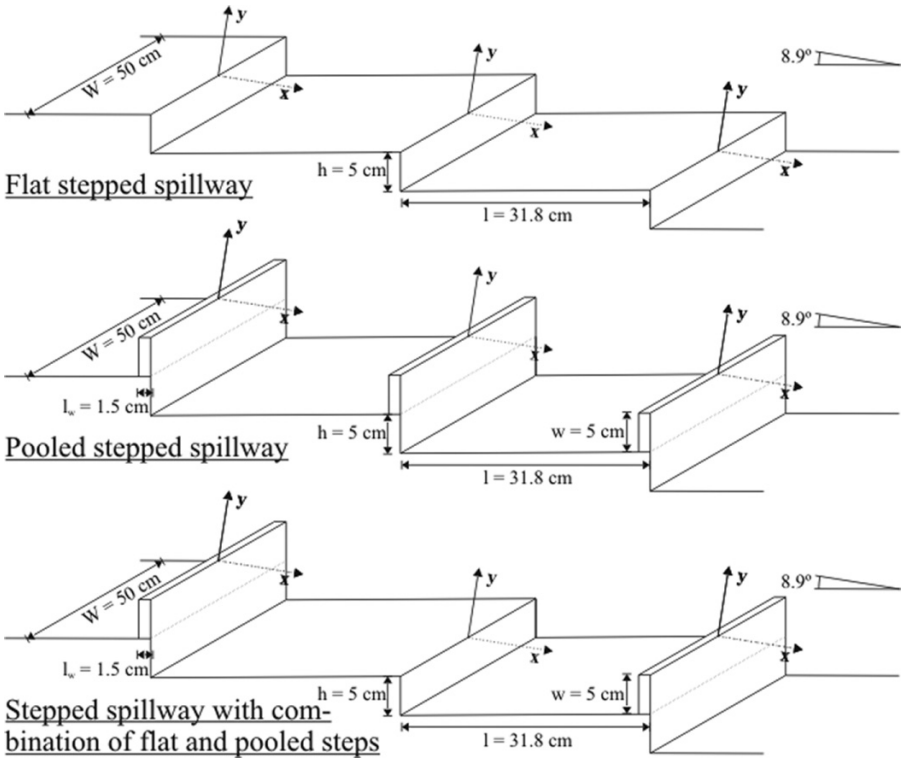

probe sensor per unit time, the time-averaged interfacial velocity V and the turbulence intensity Tu calculated based upon some cross-correlation analyses, and the air/water chord size distributions.

Experimental configurations and flow conditions

Three different stepped spillway configurations were investigated (Fig. 1). These were a stepped waterway equipped with flat horizontal steps; the pooled stepped chute with weir height w = 0.05 m and pool weir length (i.e., thickness) l_w = 0.015 m; and the third configuration was a stepped channel with a combination of flat and pooled steps (Fig. 1).

The air–water flow measurements were conducted for a broad range of discharges ($0.018 < Q < 0.117$ m^3/s) at several step edges downstream of the inception point of free-surface aeration (Table 1 and Appendix A). Table 1 summarizes the experimental flow conditions. Some results are presented in a tabular format for the three investigated configurations in Appendix A.

Air–water flow patterns

The basic flow regimes were inspected visually for discharges ranging from 0.002 m^3/s $\le Q \le 0.117$ m^3/s on the three stepped spillway configurations (Figs. 1 and 2). Figure 2 presents some photographs of the air–water flows.

On the waterway with flat horizontal steps, the flow propagated in a succession of free-falling jet and small hydraulic jump on each step for $d_c/h < 0.95$ where d_c is the critical flow depth and h the vertical step height. The flow was aerated from the first step edge and all along the stepped spillway. The present observations were typical of nappe flow on flat slope stepped spillways with comparable channel slope (Chanson and Toombes 1997; El-Kamash et al. 2005; Toombes and Chanson 2008). For dimensionless flow rates $0.95 < d_c/h < 1.69$, a transition flow regime was observed. Some key features included some strong droplet splashing and irregular flow motion (Fig. 2*a*). The observations highlighted some large turbulent fluctuations as reported in earlier studies (Ohtsu and Yasuda 1997; Chanson and Toombes 2004). For the largest flow rates ($1.69 < d_c/h$), a skimming flow regime took place. At the upstream end, the flow was a clear water flow. Once the outer edge of the turbulent boundary layer reached the free-surface, the free-surface aeration occurred. Further downstream, an air–water flow mixture was seen while the pseudo free-surface was basically parallel to the pseudo-bottom formed by the step edges. Some stable recirculation was present in the step cavities and some water droplets were ejected above the flow.

On the pooled stepped chute, a nappe flow regime was observed for $d_c/h < 1.08$. At each weir edge, the water took off as a free-falling jet impacting into the following water-filled pool. Air was entrained at the plunge point. For dimensionless flow rates $1.08 < d_c/h < 1.76$, a transition flow regime was observed and the flow became instable. Some flow instabilities were present including some self-induced jump waves (Thorwarth 2008; Felder and Chanson 2012). The jump waves had frequencies of about 0.25–0.4 Hz and were accompanied by some irregular appearance of hydraulic jump at the downstream end of the pool. Other forms of instabilities included some cyclic pulsations in the first step cavity with a lower frequency about 0.125–0.167 Hz (Fig. 3). It appeared that only about half of the jump waves were induced by flow pulsations in the first step cavity. The first four shots show the formation of the jump while the last two shots illustrate the jump disappearance (Fig. 3). Further irregular cavity ejections and recirculation motion were observed in transition and skimming flows ($1.08 < d_c/h < 3.55$) with a frequency about 0.5–2 Hz.

For the largest discharges $d_c/h > 1.76$, a skimming flow regime was observed on the pooled stepped chute (Fig. 2*c*). At the upstream end of the channel, a mono-phase flow existed with a free-surface parallel to the pseudo-bottom. Visually the free-surface appeared to be less stable than in a skimming flow on the flat horizontal stepped spillway. Some strong free-surface fluctu-

Fig. 2. Photographic observations down the stepped waterway ($\theta = 8.9°$). (*a*) Nappe–transition flow regime down the chute with flat horizontal steps: $d_c/h = 0.95$, $Q = 0.016$ m^3/s, $Re = 1.28 \times 10^5$. (*b*) Transition flow regime on the stepped spillway with combination of flat and pooled steps: $d_c/h = 1.33$, $Q = 0.027$ m^3/s, $Re = 2.14 \times 10^5$. (*c*) Skimming flow regime on the pooled stepped spillway: $d_c/h = 2.66$, $Q = 0.076$ m^3/s, $Re = 6.03 \times 10^5$.

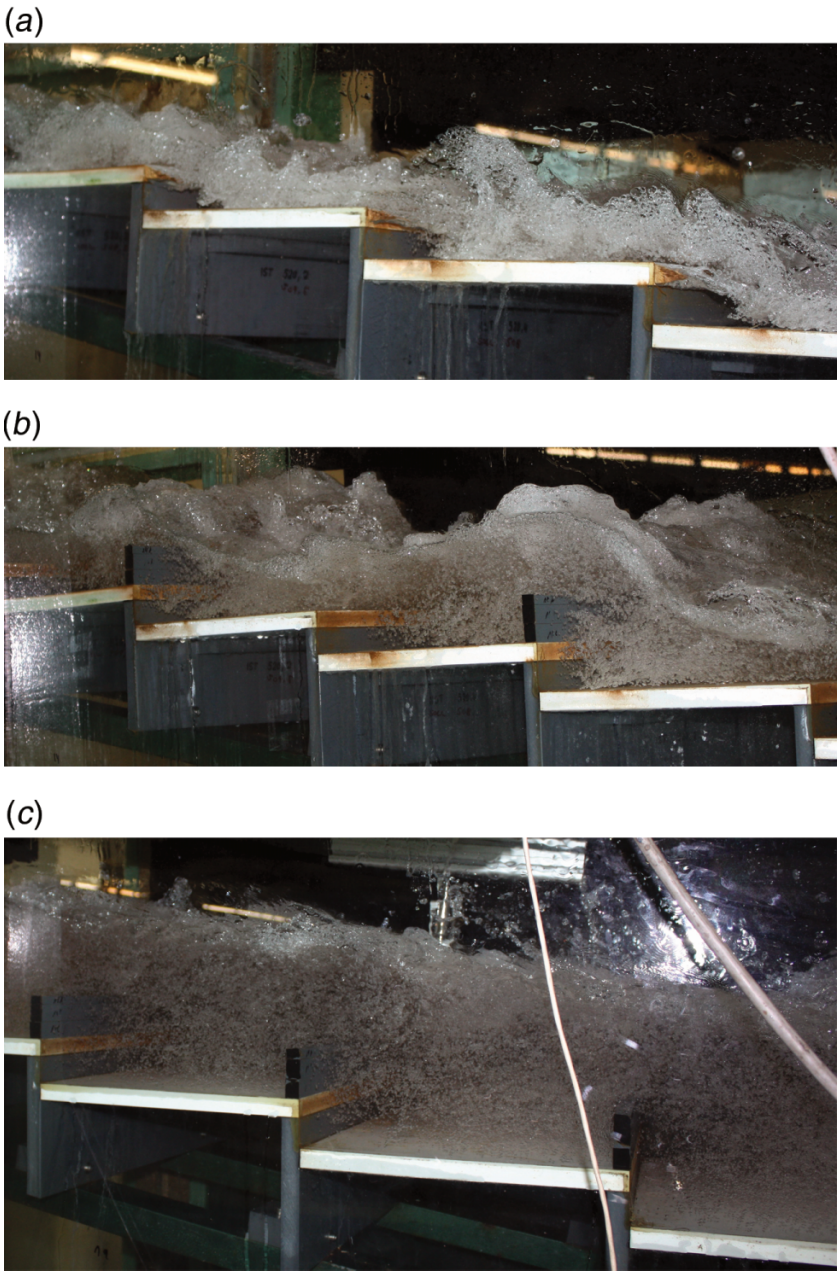

ations were visible upstream of the inception point of free-surface aeration. The fluctuation seemed to be linked with the increased step roughness induced by the weir pools. Downstream of the inception point, the flow was aerated and some instable cavity recirculation and ejection processes were seen for all skimming flow discharges in the present study. Overall the flow patterns were consistent with the observations of Thorwarth and Koengeter (2006).

On the stepped spillway configuration with combination of flat and pooled steps, a nappe flow regime was seen for dimensionless flow rates $d_c/h < 1.0$. The air–water flow cascaded downstream in a series of free-falling jets. The flow became aerated from the first step edge. A hydraulic jump took place immediately upstream of the pooled weir. For larger flow rates ($d_c/h > 1.0$), a transition flow was observed (Fig. 2*b*). The flow appeared chaotic with some strong droplet splashing at all step edges downstream of the inception point of air entrainment. Some flow instabilities were present for all flow rates, including some irregular cavity ejection and recirculation processes as well as some instationary free-surface waves. Within the experimental flow conditions investigated herein ($d_c/h < 3.55$) no skimming flow regime was seen. The visual observations were overall consistent with those of Kökpinar (2004) down a stepped chute with slope $\theta = 30°$ equipped with a combination of flat and pooled steps. Kökpinar reported a change from transition to skimming flows for a dimensionless flow rate significantly larger than that observed on flat and pooled stepped spillways.

Fig. 3. Pulsating flow in the first step cavity downstream of the broad-crested weir in the transition flow regime — Flow conditions: $d_c/h = 1.08$, $Q = 0.020$ m^3/s, $Re = 1.56 \times 10^5$ — Chronological order from left to right, top to bottom.

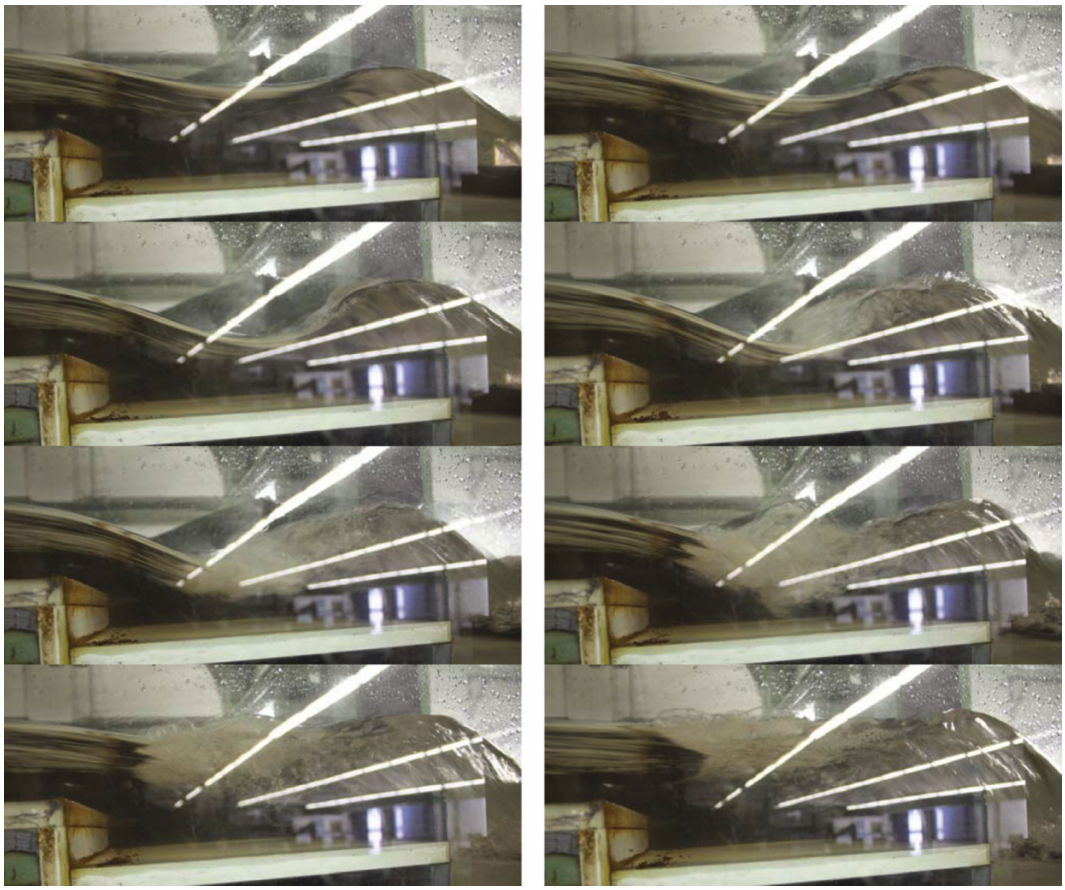

Air–water flow properties at step edges

The air–water flow properties were systematically measured for all three configurations at several step edges downstream of the inception point of free-surface aeration (Appendix A).

The vertical distributions of void fractions showed some typical S-shape distributions for all experiments (Fig. 4). In Fig. 4, some typical void fraction distributions are shown for the three stepped configurations at several consecutive step edges as functions of the dimensionless distance from the step edge $(y + w)/d_c$, where y is the distance normal to the pseudo-bottom formed by the step edges and measured from the edges of the flat steps. For the smaller flow rates, the void fraction distributions were very close between all stepped configurations, but for the vertical offset by w/d_c induced by the pool height (data not shown for conciseness). For the larger flow rates, the void fraction distributions on the stepped spillway with combination of flat and pooled steps differed from those on both flat and pooled steps (Fig. 4). The data implied different aeration levels between flat and pooled steps. Some differences were possibly linked with the different definition of $y = 0$ for the pooled and flat steps. More changes were also observed between the different step types, especially for the larger discharges (Fig. 4*b*). On the flat and pooled stepped waterways, the void fraction distributions were in qualitative agreement for all measured steps. Similarly the shapes of the void fraction distribution at consecutive step edges were unchanged for all experiments for the flat and pooled stepped spillways. In Figs. 4*a* and 4*b*, some experimental data were compared with the advective diffusion equation (Chanson and Toombes 2002*a*):

$$[1] \qquad C = 1 - \tanh^2\left[K' - \frac{y/Y_{90}}{2 \times D_o} + \frac{(y/Y_{90} - 1/3)^3}{3 \times D_o}\right]$$

where Y_{90} is the characteristic distance where $C = 0.90$, K' is an integration constant, and D_o is a function of the depth-averaged void fraction C_{mean} only.

$$[2] \qquad K' = 0.32745015 + \frac{1}{2 \times D_o} - \frac{8}{81 \times D_o}$$

$$[3] \qquad C_{mean} = \frac{1}{Y_{90}} \times \int_0^{Y_{90}} C \times dy = 0.7622 \times [1.0434 - \exp(-3.614 \times D_o)]$$

For all the data sets, the advective diffusion eq. [1] matched well the experimental data as illustrated in Fig. 4.

For a given stepped configuration, the bubble count rate distributions showed close results for all discharges. Some differences in terms of bubble count rate distributions were observed between flat and pooled steps for the combination of flat and pooled steps. The differences were the largest for the smaller flow rates (Fig. 5), while the bubble count rate distributions for the largest flow rates were close to those on both flat and pooled stepped chutes. Some typical dimensionless distributions of bubble count rates are illustrated in Fig. 5 as functions of $(y + w)/d_c$ for several consecutive step edges for all three stepped configurations. The

Fig. 4. Void fraction distributions on the stepped spillways with flat, pooled, and combination of flat and pooled steps ($\theta = 8.9°$) — Comparison with eq. [1]. (*a*) $d_c/h = 2.3$, $Q = 0.061$ m³/s, $Re = 4.85 \times 10^5$. (*b*) $d_c/h = 3.55$, $Q = 0.117$ m³/s, $Re = 9.30 \times 10^5$.

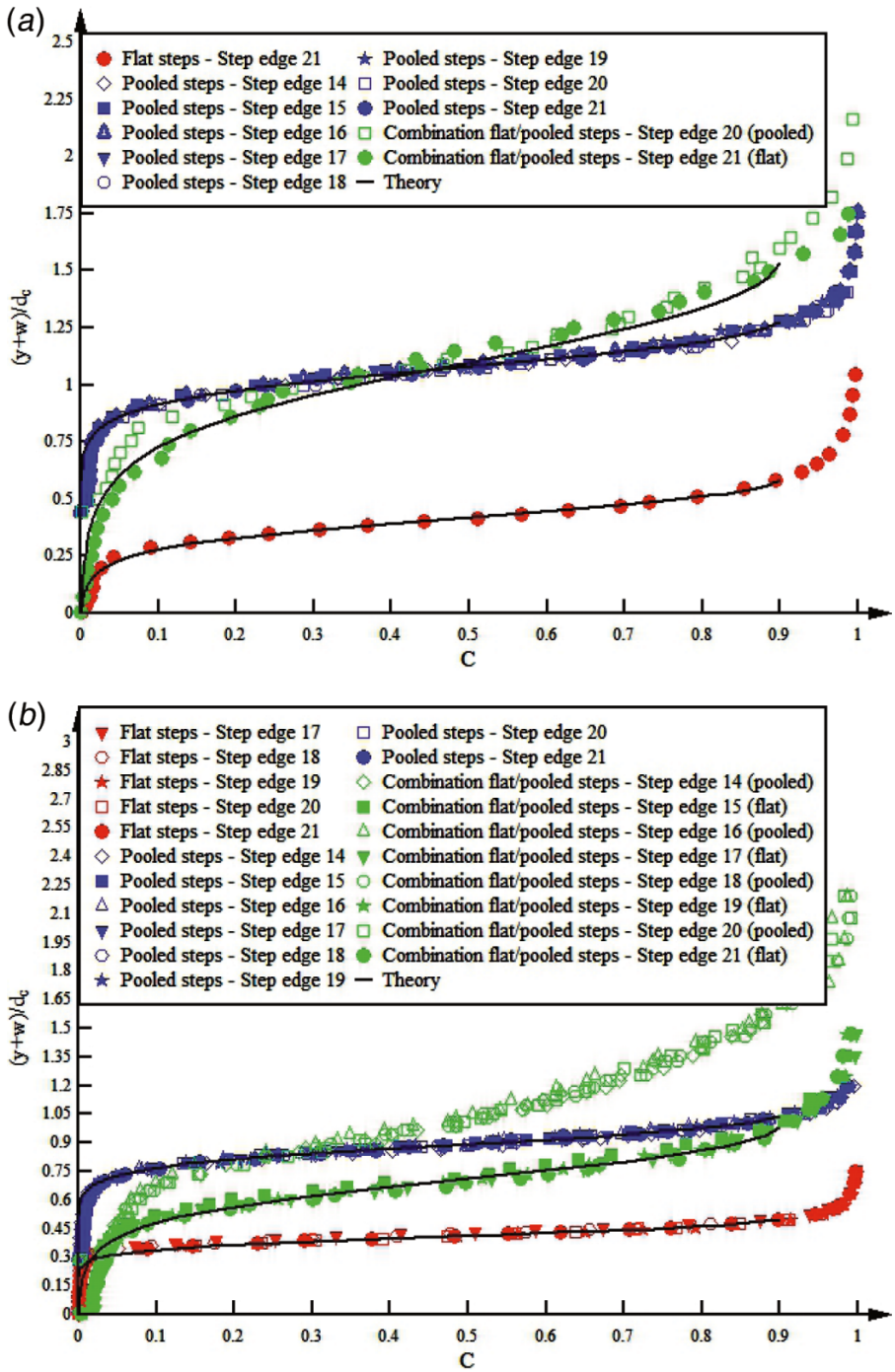

comparison of all three stepped configurations highlighted the largest bubble count rates on the flat stepped spillway for a given flow rate, within the investigated flow conditions. For the smallest flow rates, the combination of flat and pooled steps presented the smallest bubble count rates while, for the largest discharges, the pooled stepped spillway configuration had the smallest data. With increasing discharge the differences between all configurations became smaller (data not shown).

Some typical interfacial velocity distributions are presented in Fig. 6 in which some data for all three configurations are presented as functions of $(y + w)/d_c$. Qualitatively, a good agreement was achieved between flat and pooled stepped spillway data in terms of the velocity profile shape, as well as for the pooled step data on the configuration with combination of flat and pooled steps (Fig. 6). For all discharges, these data collapsed reasonably well into a self-similar power law:

$$[4] \qquad \frac{V}{V_{90}} = \left(\frac{y}{Y_{90}}\right)^{1/N} \quad 0 \le y/Y_{90} \le 1$$

where V_{90} is the characteristic air–water velocity at $y = Y_{90}$ and $C = 0.90$. The value of the exponent $1/N$ may vary from one step edge to the next one for a given flow rate, with on average $N = 10$. In the

Fig. 5. Dimensionless bubble count rate distributions on the stepped spillways with flat, pooled, and combination of flat and pooled steps (θ = 8.9°) — Flow conditions: d_c/h = 1.7, Q = 0.039 m³/s, Re = 3.10 × 10⁵.

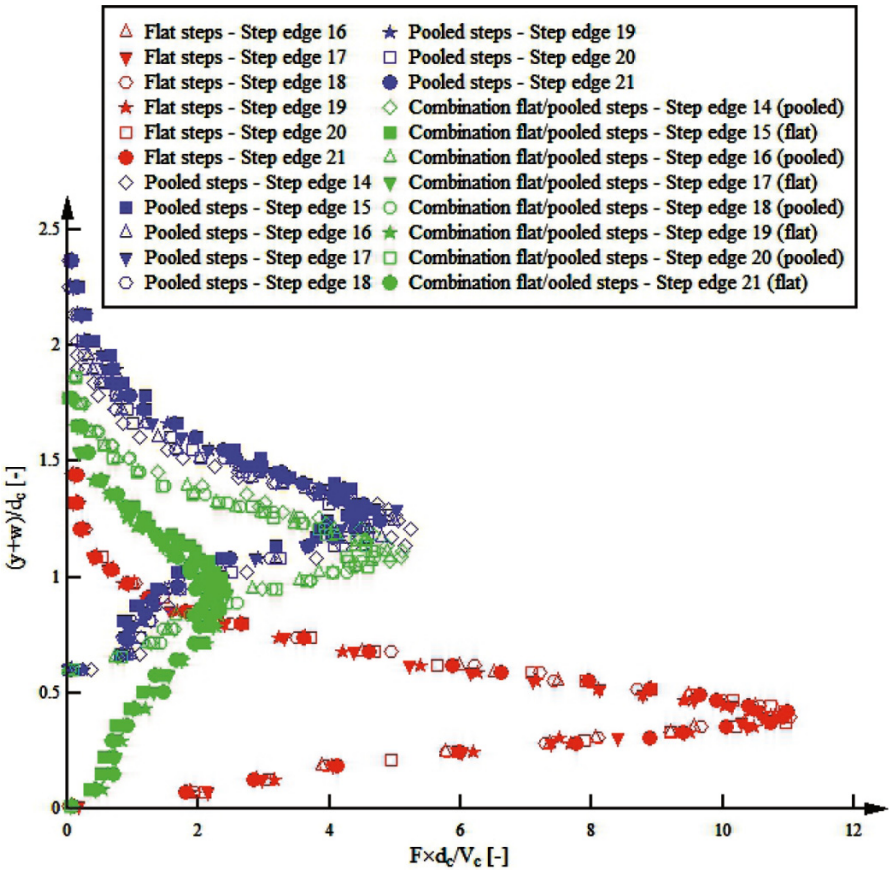

upper flow region ($y/Y_{90} > 1$), the velocity distributions had a quasi-uniform profile:

$$[5] \qquad \frac{V}{V_{90}} = 1 \quad 1 < y/Y_{90}$$

For the flat and pooled stepped spillway configurations, the data were in close agreement with eqs. [4] and [5] as illustrated in Fig. 6. Some data scatter was seen for the pooled steps on the spillway configuration with combination of flat and pooled steps, which might reflect some rapid flow distributions between flat steps and pooled steps. That is, on the flat steps of the combined flat–pooled stepped configuration, the interfacial velocity distribution exhibited a distribution shape closer to those observed at the impact of nappe flow jets and in transition flows (Chanson and Toombes 2004; Toombes and Chanson 2008) (Fig. 6).

Quantitatively, the velocity data showed some marked differences between flat and pooled stepped waterways (Fig. 6). The largest interfacial velocities V/V_c were observed for the flat stepped spillway. The magnitudes of V/V_c for the stepped spillways with pooled steps and with combination of pooled and flat steps were close and about 30% smaller than the flat stepped spillway velocity data (Fig. 6).

On the flat stepped chute, the turbulence level distributions were qualitatively and quantitatively comparable to earlier findings on flat stepped spillways with maximum values of up to 150% in the intermediate flow region (Carosi and Chanson 2008; Felder and Chanson 2009). Some typical distributions of turbulence intensity Tu are illustrated in Fig. 7 for all experimental configurations. The distributions of turbulence intensity showed however some very large turbulence levels for the pooled stepped chute and for the waterway with combination of pooled and flat steps. That is, maximum values of up to 500%–900% were observed in the intermediate flow region ($0.3 < C < 0.7$) (Fig. 7). Such very high turbulence intensity levels were discussed by Felder and Chanson (2012) who demonstrated that the instationary processes on the pooled stepped spillway configurations contributed significantly to the turbulent kinetic energy and that the turbulent intensity data included a large energy component in the slow hydrodynamic fluctuations, while the turbulent motion component was much smaller.

For all investigated flow conditions (Appendix A), similar air and water chord sizes were recorded in the bubbly flow and spray regions respectively for the flat and pooled stepped spillways (data not shown). The chord size probability distribution functions (pdfs) were skewed with a preponderance of small particle sizes compared to the mean, and the pdf data followed closely some log-normal distributions. The chord size mode was typically between 0.5 and 2 mm. Some differences were visible for the stepped spillway configuration with combination of flat and pooled stepped spillways. For the larger flow rates, a larger amount of small air bubble chord sizes was observed.

Flow resistance and turbulent energy dissipation

On a stepped chute, the water flows were characterised by significant form losses and energy dissipation. The rate of energy dissipation $\Delta H/H_{max}$ and residual head H_{res} were calculated herein at the last two steps edges of the stepped waterway based upon the air–water flow measurements (Fig. 8). Note that H_{max} is the upstream total head defined as

$$[6] \qquad H_{max} = \frac{3}{2} \times d_c + \Delta z_o$$

Fig. 6. Dimensionless interfacial velocity distributions on the stepped spillways with flat, pooled, and combination of flat and pooled steps (θ = 8.9°) — Flow conditions: d_c/h = 3.3, Q = 0.105 m³/s, Re = 8.34 × 10⁵.

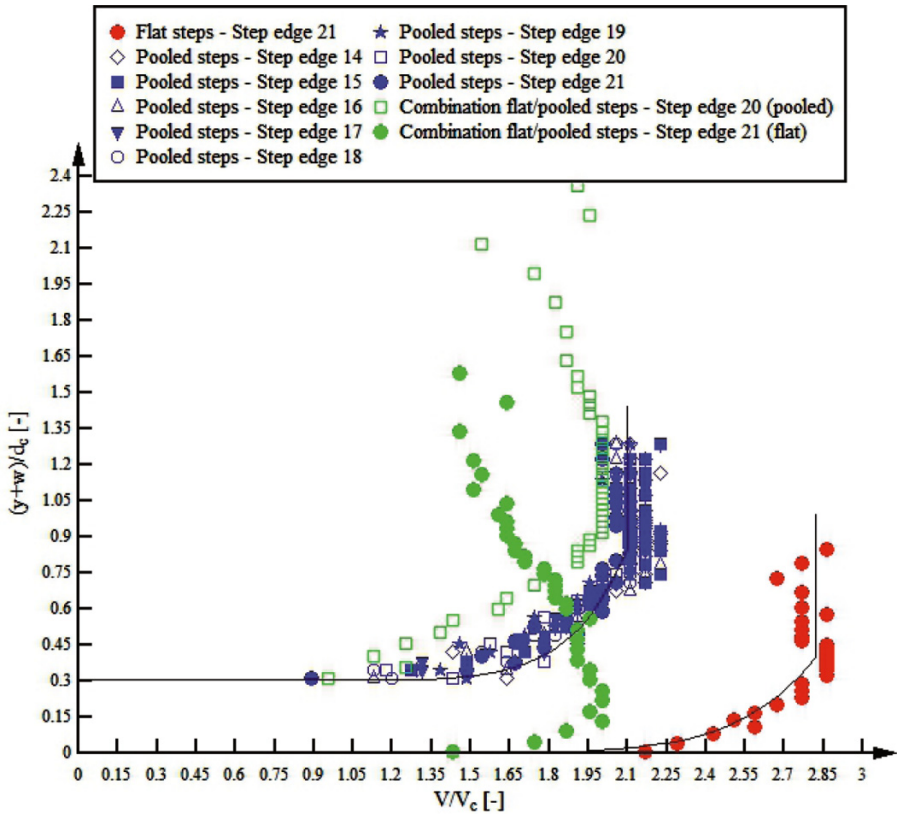

with Δz_o the drop in bed elevation from the weir crest. The total head loss was: $\Delta H = H_{max} - H_{res}$, where H_{res} is the residual head estimated as

$$[7] \quad H_{res} = d \times \cos\theta + \frac{U_w^2}{2 \times g} + w = \int_0^{Y_{90}} (1 - C) \times \cos\theta \times dy + \frac{q^2}{2 \times g \times \left(\int_0^{Y_{90}} (1 - C) \times dy \right)^2} + w$$

where d is the equivalent clear water flow depth, U_w the flow velocity ($U_w = q/d$), and q is the water discharge per unit width. The complete results in terms of residual energy are detailed in Appendix A.

The rate of energy dissipation for the three configurations is illustrated in Fig. 8*a* for the last two step edges as a function of the dimensionless drop in elevation $\Delta z_o/d_c$. The comparison between flat and pooled stepped chute performances showed a larger rate of energy dissipation on the pooled step configurations (Fig. 8*a*). The energy dissipation rate on the flat stepped waterway was the lowest of all three configurations for all flow rates. The results in terms of residual head are presented in Fig. 8*b*. On the flat stepped spillway, the dimensionless residual energy was the largest, nearly independent of the flow rate: i.e., $H_{res}/d_c \approx 3.25$. The residual head on the pooled stepped spillway was almost constant; $H_{res}/d_c \approx 2.25$ on average. Overall the residual head was the smallest for the combined configuration tending to a residual head for the largest flow rates of $H_{res}/d_c \approx 1.7$ to 1.9, although this data set presented some scatter (Fig. 8*b*).

The present data were further compared with the re-analyses of air–water flow measurements on flat slope stepped waterways (Chanson and Toombes 2002*b*; Thorwarth 2008). The present results were qualitatively and quantitatively comparable to these earlier findings, although Chanson and Toombes (2002*b*) investigated only flat steps with a milder slope (θ = 3.4°, h = 0.0715 and 0.143 m), while Thorwarth (2008) studied a smaller range of flow rates (θ = 8.9°, h = 0.05 m).

The flow resistance on stepped waterways was characterised by significant form losses caused by the steps. Following common practice (Rajaratnam 1990; Chanson et al. 2002), the Darcy–Weisbach friction factor was used to quantify the dimensionless boundary shear stress in stepped spillway flows. The flow resistance was deduced herein from the total head line slope. Figure 9*a* shows some typical longitudinal variation of the total head at the downstream end of the spillway for several consecutive step edges. The results illustrate the non-uniform nature of the flow induced by the alternation of flat and pooled steps. The Darcy–Weisbach friction factor was estimated from the measured air–water flow properties

$$[8] \quad f_e = \frac{8 \times \tau_0}{\rho_w \times U_w^2} = \frac{8 \times g \times S_f \times \left(\int_{y=0}^{Y_{90}} (1 - C) dy \right)}{U_w^2} = \frac{8 \times g \times S_f \times d}{U_w^2}$$

where f_e is the friction factor of the air–water flow, S_f is the friction slope: $S_f = -\partial H/\partial x$, H is the total head, and x is the distance in flow direction. Note that the Darcy–Weisbach friction factor for the stepped waterway with combination of flat and pooled steps was calculated by averaging the friction factors calculated for the flat

Fig. 7. Turbulence intensity distributions on the stepped spillways with flat, pooled, and combination of flat and pooled steps (θ = 8.9°) — Flow conditions: d_c/h = 2.66, Q = 0.076 m³/s, Re = 6.03 × 10⁵.

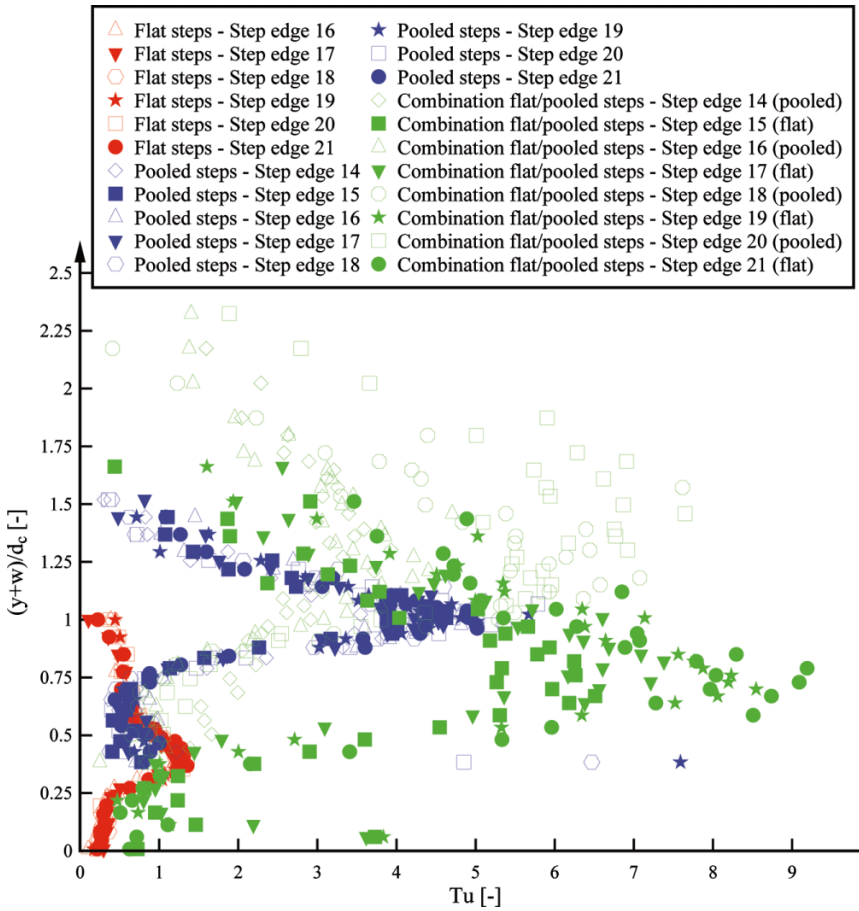

Fig. 8. Rate of energy dissipation and residual head on flat and pooled stepped waterways — Comparison between flat and pooled stepped configuration data (θ = 8.9°) and the re-analyses of the data of Chanson and Toombes (2002*b*) (θ = 3.4°) and Thorwarth (2008) (θ = 8.9°). (*a*) Dimensionless rate of energy dissipation at the chute downstream end. (*b*) Dimensionless residual head at the chute downstream end — Same legend as in Fig. 8*a*.

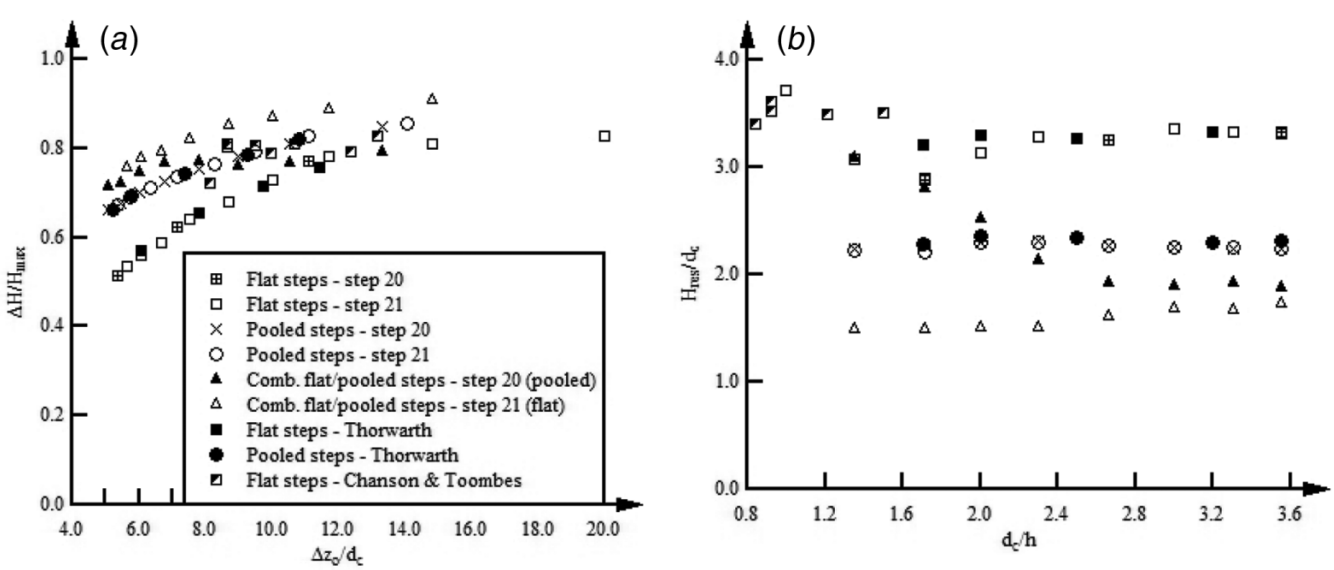

Fig. 9. Flow resistance on flat and pooled stepped waterways (*a*) Total head line at the downstream end of the waterways — Comparison between flat and pooled stepped configuration data ($\theta = 8.9°$) — Flow conditions: $d_c/h = 2.66$, $Q = 0.076$ m³/s, $Re = 6.03 \times 10^5$. (*b*) Darcy–Weisbach friction factor for flat and pooled stepped configuration data ($\theta = 8.9°$) — Comparison with the re-analysis of the data of Chanson and Toombes (2002*b*) ($\theta = 3.4°$) and Thorwarth (2008) ($\theta = 8.9°$) — Same legend as in Fig. 8*a*.

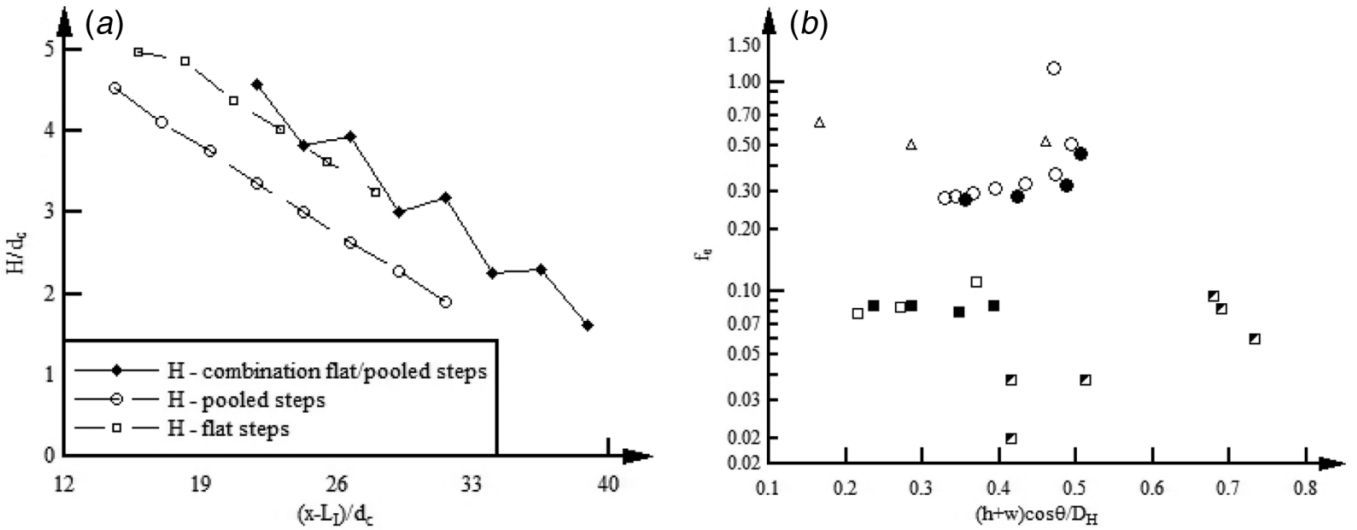

and pooled steps in this configuration. The results are presented in Fig. 9*b* as functions of the dimensionless step roughness height. In Fig. 9*b*, some re-analysed data of Thorwarth (2008) on a stepped spillway ($\theta = 8.9°$) with flat and pooled steps were included.

Overall the present results highlighted a significantly larger flow resistance on the pooled stepped waterway, together with some small friction factors on the flat stepped chutes. The results were in agreement with the re-analysed data of Thorwarth (2008) and they were consistent with the residual head data presented in Fig. 8*b*.

Conclusion

New measurements were performed on a relatively large stepped chute model with flat and pooled steps ($\theta = 8.9°$, $h = 0.05$ m). Three stepped configurations were tested systematically: a stepped chute with flat horizontal steps, a pooled stepped chute ($w/h = 1$), and a chute with an alternation of flat and pooled steps. Detailed air–water flow measurements were conducted and a comparative analysis was performed for a broad range of discharges 0.02 m³/s $\leq Q \leq 0.117$ m³/s corresponding to Reynolds numbers between 1.4×10^5 and 9.3×10^5.

The visual observations showed some typical flow patterns with nappe, transition, and skimming flows depending upon the flow rate on the flat stepped spillway. On the pooled stepped spillway configurations, some strong instabilities were observed in the transition flow regime. The self-induced instabilities were associated with instationary cavity recirculation and ejection processes as well as some strong jump waves propagating down the chute. A comparison of air–water flow properties was performed between the three configurations in terms of void fraction, bubble count rate, interfacial velocity, turbulence intensity, and chord size distributions. The void fraction distributions on flat and pooled stepped spillways were overall in agreement, but the combination of flat and pooled steps yielded some stronger aeration for a given flow rate. The interfacial velocity distributions showed largest interfacial velocities for the flat stepped spillway. The turbulence levels were significantly larger on the pooled stepped spillways and it is believed that this was caused by the flow instationarities. The results in terms of the rate of energy dissipation and residual head showed the largest rate of energy dissipation for the stepped spillway with combination of flat and pooled steps, while the largest residual head and lowest rate of energy dissipation were observed for the flat stepped waterway. The Darcy–Weisbach friction factor data showed the smallest values for the flat stepped spillway.

While the stepped chute configurations with pooled steps yielded the largest rate of energy dissipation, these geometries were affected by some flow instabilities and unsteady flow processes for a range of flow rates. These configurations should not be regarded as an optimum design because the instabilities might cause an unsafe operation of the structure.

Acknowledgements

The authors acknowledge the assistance of Mr. Christopher Fromm with some physical work. They thank Dr. Mehmet A. Kökpinar (Turkey) for his helpful comments, and Professor Holger Schüttrumpf (IWW, RWTH Aachen University, Germany) for providing the experimental facility and instrumentation. The first writer acknowledges the financial support through a University of Queensland research scholarship and a Graduate School International Travel Award. The financial support of the Australian Research Council is acknowledged (ARC DP0878922 & DP120100481).

References

André, S. 2004. High velocity aerated flows on stepped chutes with macro-roughness elements. Ph.D. thesis, Laboratoire de Constructions Hydrauliques LCH, EPFL, Lausanne, Switzerland, 272 pages.

Bung, D.B. 2009. Zur selbstbelüfteten Gerinneströmung auf Kaskaden mit gemäßigter Neigung. Ph.D. thesis, Lehr- und Forschungsgebiet Wasserwirtschaft und Wasserbau, Bergische Universitaet Wuppertal, Germany [in German].

Carosi, G., and Chanson, H. 2008. Turbulence characteristics in skimming flows on stepped spillways. Canadian Journal of Civil Engineering, **35**(9): 865–880. doi:10.1139/L08-030.

Chamani, M.R., and Rajaratnam, N. 1999. Characteristics of skimming flow over stepped spillways. Journal of Hydraulic Engineering, **125**(4): 361–368. doi:10.1061/(ASCE)0733-9429(1999)125:4(361).

Chanson, H. 1993. Stepped spillway flows and air entrainment. Canadian Journal of Civil Engineering, **20**(3): 422–435. doi:10.1139/l93-057.

Chanson, H. 2001. The Hydraulics of Stepped Chutes and Spillways. Balkema, Lisse, The Netherlands. 418 pp.

Chanson, H., and Toombes, L. 1997. Energy Dissipation in Stepped Waterway. *In* Proceedings of 27th IAHR Biennial Congress, San Francisco, USA, Vol. D. *Edited by* F.M. Holly, Jr. and A. Alsaffar. pp. 595–600.

Chanson, H., and Toombes, L. 2002*a*. Air-water flows down stepped chutes: turbulence and flow structure observations. International Journal of Multiphase Flow, **28**(11): 1737–1761. doi:10.1016/S0301-9322(02)00089-7.

Chanson, H., and Toombes, L. 2002*b*. Energy dissipation and air entrainment in a stepped storm waterway: an experimental study. Journal of Irrigation and

Drainage Engineering, **128**(5): 305–315. doi:10.1061/(ASCE)0733-9437(2002)128:5(305).
Chanson, H., and Toombes, L. 2004. Hydraulics of stepped chutes: the transition flow. Journal of Hydraulic Research, **42**(1): 43–54. doi:10.1080/00221686.2004.9641182.
Chanson, H., Yasuda, Y., and Ohtsu, I. 2002. Flow resistance in skimming flows and its modelling. Canadian Journal of Civil Engineering, **29**(6): 809–819. doi:10.1139/l02-083.
El-Kamash, M.K., Loewen, M.R., and Rajaratnam, N. 2005. An experimental investigation of jet flow on a stepped chute. Journal of Hydraulic Research, **43**(1): 31–43. doi:10.1080/00221680509500109.
Felder, S., and Chanson, H. 2009. Turbulence, dynamic similarity and scale effects in high-velocity free-surface flows above a stepped chute. Experiments in Fluids, **47**(1): 1–18. doi:10.1007/s00348-009-0628-3.
Felder, S., and Chanson, H. 2012. Air-Water Flow Measurements in Instationary Free-Surface Flows: a Triple Decomposition Technique. Hydraulic Model Report No. CH85/12, School of Civil Engineering, The University of Queensland, Brisbane, Australia. 161 pp.
Felder, S., Fromm, C., and Chanson, H. 2012. Air Entrainment and Energy Dissipation on a 8.9° Slope Stepped Spillway with Flat and Pooled Steps. Hydraulic Model Report No. CH86/12, School of Civil Engineering, The University of Queensland, Brisbane, Australia. 80 pp.
Kökpinar, M.A. 2004. Flow over a stepped chute with and without macro-roughness elements. Canadian Journal of Civil Engineering, **31**(5): 880–891. doi:10.1139/l04-059.
Ohtsu, I., and Yasuda, Y. 1997. Characteristics of Flow Conditions on Stepped Channels. Proceedings of the 27th IAHR Biennial Congress, San Francisco USA, Theme D. pp. 583–588.
Rajaratnam, N. 1990. Skimming flow in stepped spillways. Journal of Hydraulic Engineering, **116**(4): 587–591. doi:10.1061/(ASCE)0733-9429(1990)116:4(587).
Ruff, J.F., and Frizell, K.H. 1994. Air Concentration Measurements in Highly-Turbulent Flow on a Steeply-Sloping Chute. Proceedings of Hydraulic Engineering Conference, American Society of Civil Engineers, Buffalo, USA. Vol. 2, pp. 999–1003.
Thorwarth, J. 2008. Hydraulisches Verhalten der Treppengerinne mit eingetieften Stufen – Selbstinduzierte Abflussinstationaritäten und Energiedissipation. Hydraulics of Pooled Stepped Spillways – Self-induced Unsteady Flow and Energy Dissipation. Ph.D. thesis, University of Aachen, Germany. [In German].
Thorwarth, J., and Koengeter, J. 2006. Physical Model Tests on a Stepped Chute with Pooled Steps. Investigations of Flow Resistance and Flow Instabilities. Proceedings of the International Symposium on Hydraulic Structures, IAHR, Ciudad Guayana, Venezuela. *Edited by* A. Marcano and A. Martinez. pp. 477–486.
Toombes, L., and Chanson, H. 2008. Flow patterns in nappe flow regime down low gradient stepped chutes. Journal of Hydraulic Research, **46**(1): 4–14. doi:10.1080/00221686.2008.9521838.

List of symbols

C	void fraction defined as the volume of air per unit volume (also called air concentration)
C_{mean}	depth averaged air concentration defined as: $(1 - Y_{90}) \times C_{mean} = d$
D_o	dimensionless diffusivity term
d	equivalent clear-water depth (m) defined as: $d = \int_0^{Y_{90}} (1 - C) \times dy$
d_c	critical flow depth (m)
F	bubble count rate (Hz) defined as the number of bubbles detected by the probe sensor per second
f_e	Darcy friction factor for air–water flow
g	gravity constant (m/s²) or acceleration of gravity
H	total head (m)
H_{max}	upstream head (m) above spillway toe
H_{res}	residual head (m)
h	height of steps (m) (measured vertically)
K'	integration constant
L	length (m) of facility
l	horizontal length of steps (m)
l_w	pool weir length (i.e., thickness) (m)
Q	water discharge (m³/s)
q	water discharge per unit width (m²/s): $q = Q/W$
Re	flow Reynolds number defined in terms of the hydraulic diameter
S_f	friction slope: $S_f = -\partial H/\partial x$
Tu	turbulence intensity: $Tu = u'/V$
U_w	equivalent clear water flow velocity (m/s): $U_w = q/d$
u'	root mean square of longitudinal component of turbulent velocity (m/s)
V	interfacial velocity (m/s)
V_c	critical flow velocity (m/s)
V_{90}	characteristic velocity (m/s) where $C = 0.90$
W	chute width (m)
w	weir height in pooled stepped spillway configuration (m), also called pool height
x	longitudinal distance (m)
Y_{90}	characteristic depth (m) where the air concentration is 90%
y	distance (m) from the pseudo-bottom (formed by the step edges) measured perpendicular to the flow direction
ΔH	total head loss (m)
Δx	probe tip separation (m) in the streamwise direction
Δz	transverse separation distance (m) between sensor
Δz_o	drop (m) in bed elevation measured from the weir crest
θ	angle between the pseudo-bottom formed by the step edges and the horizontal
ρ_w	water density (kg/m³)
τ_o	boundary shear stress (Pa)
$\varnothing$	diameter (m)

Appendix A

Table A1 appears on the following page.

Table A1. Summary of air–water flow measurements on 8.9° stepped waterways (present study).

Configuration (1)	d_c/h (2)	Q [m³/s] (3)	Re (4)	Measurement at step edge (5)	Inception point step edge (6)	Flow regime (7)	f_e (8)	H_{res}/d_c [Step 20] (9)	H_{res}/d_c [Step 21] (10)
Flat stepped spillway	1.0	0.018	1.39×10^5	21	4	TRA	—	—	3.71
	1.35	0.027	2.18×10^5	21	4	TRA	—	—	3.08
	1.7	0.039	3.10×10^5	16–21	5	SK/TRA	0.111	2.875	2.90
	2.0	0.049	3.93×10^5	21	6	SK	—	—	3.13
	2.3	0.061	4.85×10^5	21	7	SK	—	—	3.28
	2.66	0.076	6.03×10^5	16–21	9 to 10	SK	0.084	3.255	3.25
	3.0	0.091	7.23×10^5	21	10 to 11	SK	—	—	3.36
	3.3	0.105	8.34×10^5	21	13 to 14	SK	—	—	3.33
	3.55	0.117	9.30×10^5	17–21	14 to 15	SK	0.078	3.33	3.315
Pooled stepped spillway	1.35	0.027	2.18×10^5	14–21	3	TRA	1.175	2.23	2.23
	1.7	0.039	3.10×10^5	14–21	5	SK/TRA	0.505	2.27	2.20
	2.0	0.049	3.93×10^5	20+21	6	SK	0.362	2.30	2.295
	2.3	0.061	4.85×10^5	14–21	7	SK	0.328	2.31	2.30
	2.66	0.076	6.03×10^5	14–21	8	SK	0.310	2.27	2.27
	3.0	0.091	7.23×10^5	20+21	9	SK	0.295	2.255	2.25
	3.3	0.105	8.34×10^5	14–21	10	SK	0.286	2.25	2.25
	3.55	0.117	9.30×10^5	14–21	11	SK	0.283	2.23	2.24
Combination of flat and pooled steps	1.35	0.027	2.18×10^5	20+21	3 to 4	TRA	—	3.09	1.50
	1.7	0.039	3.10×10^5	14–21	4	TRA	0.515	2.80	1.49
	2.0	0.049	3.93×10^5	20+21	4 to 5	TRA	—	2.53	1.51
	2.3	0.061	4.85×10^5	20+21	4 to 5	TRA	—	2.13	1.50
	2.66	0.076	6.03×10^5	14–21	5	TRA	0.636	1.93	1.61
	3.0	0.091	7.23×10^5	20+21	5	TRA	—	1.89	1.69
	3.3	0.105	8.34×10^5	20+21	5	TRA	—	1.93	1.68
	3.55	0.117	9.30×10^5	14–21	5	TRA	0.503	1.88	1.73

Note: SK, skimming flow regime; TRA, transition flow regime; (—), data not available.